

# Micellization of triblock copolymers in a solvent selective for the middle block: influence of the molar mass

José R. Quintana, María D. Jáñez and Issa Katime\*

Grupo de Nuevos Materiales, Departamento de Química Física, Facultad de Ciencias, Campus de Leioa, Universidad del País Vasco, Apartado 644, 48080 Bilbao, Spain  
(Revised 30 June 1997)

The micellization thermodynamics and micelle structural parameters for polystyrene-*b*-poly(ethylene/butylene)-*b*-polystyrene copolymers (SEBS) in *n*-octane were studied. This solvent is selective for the middle poly(ethylene/butylene) block of the copolymer. The copolymer samples have similar chemical composition and different molar mass. Standard thermodynamic functions of micellization ( $\Delta G^\circ$ ,  $\Delta H^\circ$  and  $\Delta S^\circ$ ) were determined by light scattering. All the functions showed more negative values for the SEBS copolymer with a larger molar mass. The structural parameters of micelles formed by different triblock copolymers were determined from static light scattering and viscosity measurements. Micelle molar mass, association number and viscometric hydrodynamic radius increase with the length of the copolymer chain for a constant copolymer composition; however, the radius of gyration decreases. Finally, the results found for SEBS micelles in *n*-octane are compared to those found for SEBS micelles in 4-methyl-2-pentanone. The different behaviour found supports the idea that the micelles of a triblock copolymer in a selective solvent of the middle block will show a shell formed by loops of the middle block in order that the two outer blocks go into the micelle core and even some poorly solvated outer blocks could be extended out of the micelle. © 1998 Elsevier Science Ltd. All rights reserved.

(Keywords: triblock copolymers; critical micelle concentration; micellation thermodynamics)

## INTRODUCTION

The ability of diblock and triblock copolymers to self-assemble into micelles, even in very dilute solutions, has been established for over 25 years. Most studies have been concerned with AB and BAB block copolymers in selective solvents for the B blocks. It is well known that in these cases, the block copolymer may associate in solution to form micelles as a result of different solvation of the copolymer blocks and their incompatibility<sup>1–4</sup>. The micelles consist of a relative compact core formed by the least soluble blocks surrounded by a flexible and highly swollen shell formed by the other blocks. In most cases, these micelles have a spherical shape and a narrow size distribution<sup>5,6</sup>, suggesting that the micellization follows the closed association model, which assumes a dynamic equilibrium between free copolymer chains and micelles with a determined association number. According to this model, the critical micelle concentration, CMC, is defined as the concentration at which the experimental method in use can just detect the presence of micelles in the solution when the concentration is increased at constant temperature. At concentrations above the critical micelle concentration, all the copolymer chains added to the solutions associate to form micelles.

The association phenomenon of triblock copolymers dissolved in selective solvent for the middle block is not yet well established. Whereas some authors<sup>7–9</sup> failed to detect any multimolecular association, others<sup>10–12</sup> found

well-defined micelles. The association complexity may be understood by considering that to bring the two outer blocks into the micelle core, the middle block, which forms the micelle shell, must form a loop. This implies an additional entropic penalty to the micelle formation. If this penalty is too large, some copolymer chains, placed in the micelle, might elect to have one poorly solvated outer block extending into solution. If the copolymer concentration is large enough, this outer block can form part of another micellar core or interact with another outer block which presents the same condition. Micelle aggregates would be formed in this way<sup>13</sup>. Another possible mechanism for circumventing the entropy penalty would be through the formation of a branched structure, consisting of joints of the poorly solvated outer blocks that are connected by strands of the well-solvated middle blocks of the copolymer.

A thermodynamic study of micelle formation can be carried out from the temperature dependence of the critical micelle concentration. For micelle systems with a high enough association number and a low micelle concentration, the standard Gibbs energy per mole of copolymer chain in the micellization process,  $\Delta G^\circ$ , can be expressed by

$$\Delta G^\circ \approx RT \ln(\text{CMC}) \quad (1)$$

If the association number does not depend on temperature, it follows from the above equation and the Gibbs–Helmholtz equation

$$\Delta H^\circ \approx R \frac{d \ln \text{CMC}}{dT^{-1}} \quad (2)$$

This equation allows one to determine the standard enthalpy of micellization,  $\Delta H^\circ$ . The standard entropy of

\* To whom correspondence should be addressed at: Algorta, Getxo, Avda. Basagoiti, 8-1°C, 48990 Vizcaya, Spain

micellization,  $\Delta S^\circ$ , can be calculated from the standard enthalpy and Gibbs energy.

The factors that influence the micellization process and the structural parameters of micelles include composition, structure and molar mass of the copolymer, interactions between the copolymer blocks and the solvent, copolymer concentration, temperature and preparation methods. Many studies on characterization of micelle solutions have been carried out in recent years. Few of them have paid attention to the influence of the length of the copolymer block on the micellization process for dilute solutions of AB block copolymers<sup>14-19</sup>, even fewer for solutions of ABA block copolymers in selective solvents of the A block<sup>20</sup> and, to our knowledge, none for solutions of ABA block copolymers in selective solvents of the B block.

This paper is concerned precisely with the thermodynamics of micelle formation and the structural parameters of micelles as a function of the molar mass of ABA block copolymers in dilute solutions of a selective solvent for the middle block. The investigation was carried out for three polystyrene-*b*-poly(ethylene/butylene)-*b*-polystyrene copolymers, SEBS, in *n*-octane. The three block copolymers have a similar weight percentage of polystyrene but different molar mass. *n*-Octane is a good solvent for the poly(ethylene/butylene) block and precipitant for the polystyrene blocks. In a previous paper<sup>20</sup> the micellization process of these same copolymers in 4-methyl-2-pentanone was investigated. Micelle molar mass and size increased with the length of the copolymer chain for a constant copolymer composition, but association number decreased.

## EXPERIMENTAL

### Materials and solution preparation

The polystyrene-*b*-poly(ethylene/butylene)-*b*-polystyrene triblock copolymer samples used, designated SEBS1, SEBS2 and SEBS3, are commercial products kindly provided by Shell España, S.A. The samples have been previously characterized in detail<sup>20</sup>. They are homogeneous in chemical composition and their mass average molar mass, polydispersity and styrene content are shown in *Table 1*. *n*-Octane (analytical purity grade) was used without further purification. The solvent used for light scattering measurements was filtered four times using a 0.02  $\mu\text{m}$  aluminium oxide membrane filter. All the solutions were prepared by dissolving the copolymer in *n*-octane at temperatures close to 70°C and in sealed flasks. Copolymer solutions were filtered at 60°C directly into the scattering cells using 0.2  $\mu\text{m}$  PTFE Acrodisc CR filters to clarify them. The cells were then sealed. Copolymer solutions for viscosity measurements were filtered with number 3 glass filters. Solution concentrations used to determine the critical micelle temperature, CMT, were recalculated at the CMTs. As all the used copolymer solutions were diluted, solutions

**Table 1** Characteristics of the block copolymers: mass average molar mass of the copolymer,  $M_w$ , of the polystyrene blocks,  $M_{w,PS}$ , and of the poly(ethylene/butylene) block,  $M_{w,PEB}$ , polydispersity index,  $I$ , and polystyrene weight percentage

	SEBS1	SEBS2	SEBS3
$M_w/\text{g mol}^{-1}$	60700	87300	260000
$M_{w,PS}/\text{g mol}^{-1}$	$2 \times 9100$	$2 \times 14000$	$2 \times 39000$
$M_{w,PEB}/\text{g mol}^{-1}$	42500	59400	182000
$I$	1.09	1.11	1.18
%PS by weight	30	32	30

were assumed to have the same thermal expansion coefficient as that of pure solvent.

### Viscometry

The viscosity measurements were made in a Lauda automatic Ubbelohde viscometer model Viscoboy 2, which was placed in a thermostatically controlled bath with a precision of  $\pm 0.01^\circ\text{C}$ . The viscometer was calibrated using several standard solvents and kinetic energy corrections were carried out. The data were evaluated according to Heller equations<sup>21</sup>

$$\frac{c}{\eta_{sp}} = \frac{1}{[\eta]} - k_1 c \quad (3)$$

$$\frac{c}{\ln \eta_r} = \frac{1}{[\eta]} + k'_1 c \quad (4)$$

where  $\eta_{sp}$  is the specific viscosity,  $\eta_r$  the viscosity ratio,  $[\eta]$  the intrinsic viscosity,  $k_1$  and  $k'_1$  the Huggins and Kraemer coefficients, respectively, and  $c$  the copolymer concentration.

### Static light scattering

The light scattering technique was employed to determine micellization thermodynamics and micellar structural parameters. Static light scattering measurements, SLS, were performed on a modified FICA 42000 light scattering photogoniometer. Both light source and optical block of the incident beam were replaced by a Spectra-Physics He-Ne laser, model 105, which emits vertically polarized light at 632.8 nm with a power of 5 mW. The instrument was calibrated with pure benzene taking the Rayleigh ratio at 25°C as  $12.55 \times 10^{-6} \text{ cm}^{-1}$ .

Investigations on the thermodynamics of micellization of block copolymers in organic solvents have shown that it is far more convenient experimentally to carry out measurements in which the concentration is kept constant and the scattered light intensity is monitored over a range of temperatures in order to find the critical micelle temperature, CMT, than keeping the temperature constant and varying the concentration so as to find the CMC<sup>22</sup>. The CMT of a solution at a given concentration is defined as the temperature at which the experimental method in use can just detect the presence of micelles. Thus, it has been shown<sup>23</sup> that, within the experimental error

$$\frac{d \ln \text{CMC}}{dT^{-1}} = \frac{d \ln c}{d(\text{CMT})^{-1}} \quad (5)$$

So, Eq. (2) becomes

$$\Delta H^\circ \approx R \frac{d \ln c}{d(\text{CMT})^{-1}} \quad (6)$$

Measurements of light scattered intensity were carried out at a series of temperatures within the range of 15–90°C at a scattering angle of 45° to determine critical micelle temperatures.

Light scattering measurements were taken at 11 angles between 30 and 150° for the solvent and each copolymer solution at 25° to get classical Zimm plots. The intensity of the light scattered by a dilute polymer solution may be expressed as<sup>24</sup>

$$\frac{Kc}{\Delta R(\theta)} = \frac{1}{M_w} \left( 1 + \frac{16\pi^2 n^2 R_G^2}{3\lambda_0^2} \sin^2 \left( \frac{\theta}{2} \right) \right) + 2A_2 c \quad (7)$$

where  $K$  is an optical constant,  $c$  the polymer concentration,

$\Delta R(\theta)$  the difference between the Rayleigh ratio of the solution and that of the pure solvent,  $M_w$  the mass average molar mass,  $R_G$  the  $z$ -average radius of gyration,  $n$  the solution refractive index,  $\lambda_0$  the wavelength in vacuum,  $A_2$  the second virial coefficient and  $\theta$  the scattering angle.

The extrapolation of  $kc/\Delta R(\theta)$  at zero angle by means of a mean-square linear fit allows us to know the apparent radius of gyration,  $R_{app}$ , from the slope and the apparent mass,  $M_{app}$ , from the ordinate for a given concentration.

#### Refractive index increment

The refractive index increment,  $dn/dc$ , must be known to estimate  $M_w$  and  $R_G$ . The refractive index increment of the copolymer solutions were measured using a Brice-Phoenix differential refractometer equipped with a He-Ne laser as light source (Spectra Physics, model 156, 632.8 nm and power of 1 mW). The instrument was calibrated with solutions of highly purified NaCl. The  $dn/dc$  values of the three SEBS copolymers in *n*-octane at 25° were equal (0.1289).

## RESULTS AND DISCUSSION

It was found that whereas copolymers SEBS1 and SEBS2 form stable solutions in *n*-octane, SEBS3 is not dissolved or forms clusters which can be seen with the naked eye even at concentrations as low as  $8 \times 10^{-5} \text{ g cm}^{-3}$ . We failed to find SEBS3 micelles in solutions of *n*-octane and then further investigations were focussed on SEBS1 and SEBS2 solutions. Light scattering and viscometry were employed to investigate the behaviour of SEBS1 and SEBS2 in *n*-octane.

#### Static light scattering

Static light scattering measurements were mainly performed on solutions of both copolymers, whose concentrations ranged between  $5 \times 10^{-4}$  and  $9 \times 10^{-3} \text{ g cm}^{-3}$ , in *n*-octane at 25°C. Plots of the reciprocal apparent mass,  $1/M_{app}$ , as a function of concentration for both copolymers are shown in Figure 1. The concentration dependences of  $M_{app}$  show a curvature at the lower concentrations suggesting that the free copolymer chains and micelles coexist in the solutions at similar concentrations. At higher concentrations the concentration dependence becomes linear suggesting that under these experimental conditions micelle formation is overwhelmingly favoured and the average molar mass,  $M_w$ , determined from the double extrapolation to zero angle and concentration could be considered as the micelle molar mass. Standard Zimm plots were found at concentrations higher than  $5 \times 10^{-3} \text{ g cm}^{-3}$  for both copolymers (Figure 2). Mass average molar masses, second virial coefficients and radii of gyration were determined from the Zimm plots and are shown in Table 2.

The low molar mass and association number that SEBS1 and SEBS2 micelles show in *n*-octane contrast with the high values that the same copolymer samples show in 4-methyl-2-pentanone<sup>20</sup>. This solvent is selective of the polystyrene blocks. Therefore, the low association number of the copolymers in *n*-octane can be attributed to the difficulty that the copolymer chains find to form a micelle with a core constituted by the outer blocks. The micelle must have loops formed by the middle block and even some polystyrene blocks will be out of the micelle structure. The less order that this kind of micelle will have will not allow a large number of chains to become part of the micelle. Whereas the micelle association number of the SEBS copolymers in

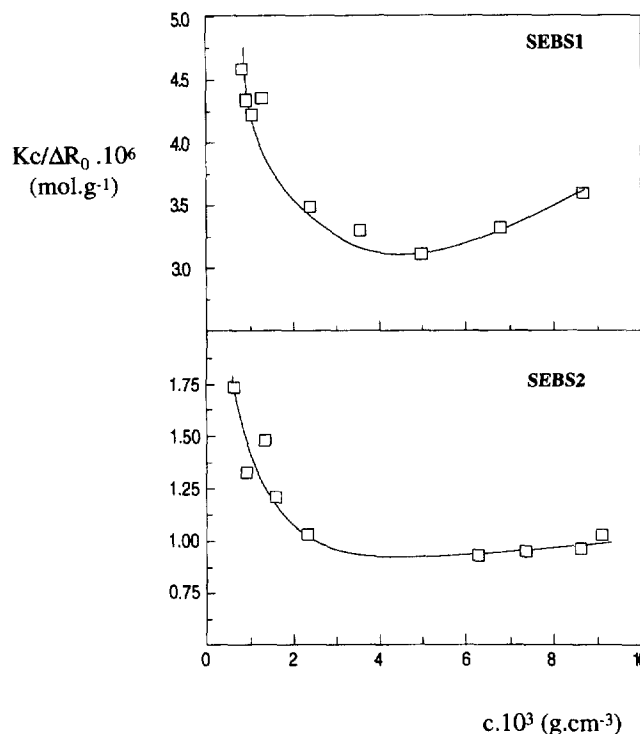


**Figure 1** Concentration dependence of  $Kc/\Delta R_0 = 1/M_{app}$  for the copolymers SEBS1 and SEBS2 in *n*-octane at 25°C

**Table 2** Mass average molar mass,  $M_w$ , association number,  $N$ , second virial coefficient,  $A_2$ ,  $z$ -average radius of gyration,  $R_G$ , intrinsic viscosity,  $[\eta]$ , degree of solvation,  $\xi$ , and radius of the equivalent hydrodynamic sphere,  $R_h$ , for SEBS copolymer micelles in *n*-octane at 25°C

	SEBS1	SEBS2
$M_w \times 10^{-5}/\text{g mol}^{-1}$	3.86	11.60
$N$	6	13
$A_2 \times 10^5/\text{mol cm}^3 \text{ g}^{-2}$	5.63	0.61
$R_G/\text{nm}$	39	32
$[\eta]/\text{cm}^3 \text{ g}^{-1}$	59.9	68.0
$\xi$	21.6	24.7
$R_h/\text{nm}$	15	23

4-methyl-2-pentanone decreases as the copolymer molar mass increased<sup>20</sup>, in *n*-octane the association number increases with the copolymer molar mass.

For both copolymers the second virial coefficient shows small and positive values (Table 2), which can be explained by taking into account the fact that the solvent is rejected from the micelle core giving rise to less unfavourable contacts between the PS segments and the *n*-octane molecules. The protective shell of solvated PEB segments hinders long-range PS segment-PS segment interactions in most cases.

The radii of gyration,  $R_G$ , were calculated from the angle dependences of  $kc/\Delta R$  at nil concentration. The values, shown in Table 2, are apparent, lower than the true ones due to the core-shell of the scattering particles, with the polystyrene core having a larger refractive index increment in *n*-octane than the poly(ethylene/butylene) shell.

The  $R_G$  values found are remarkably high if they are compared to those shown by SEBS micelles in 4-methyl-2-pentanone<sup>20</sup>. In this system where the micelle shell consists of the end copolymer blocks, micelles with a molar mass of  $10 \times 10^6 \text{ g mol}^{-1}$  had a radius of gyration of 16 nm. However, the micelles with a shell formed by the middle

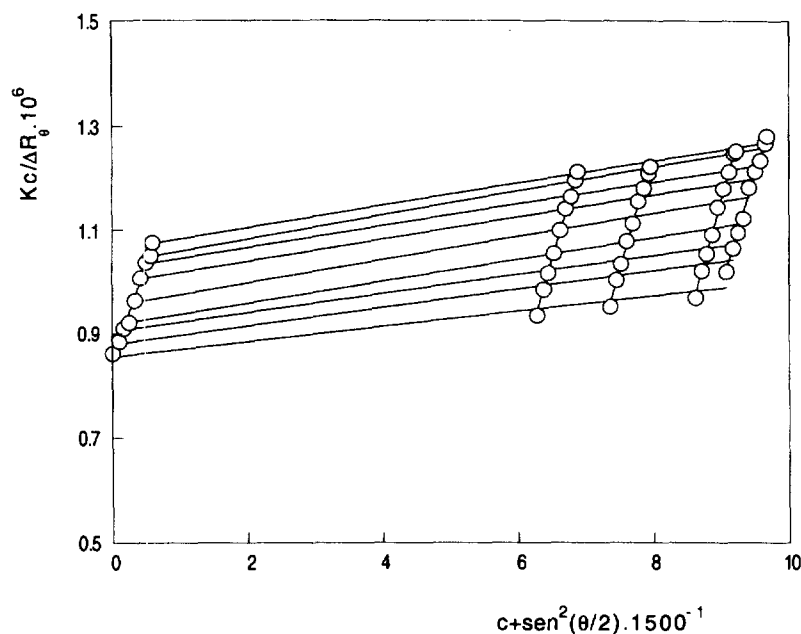


Figure 2 Zimm plot for micellar solutions of SEBS2 in *n*-octane at 25°C

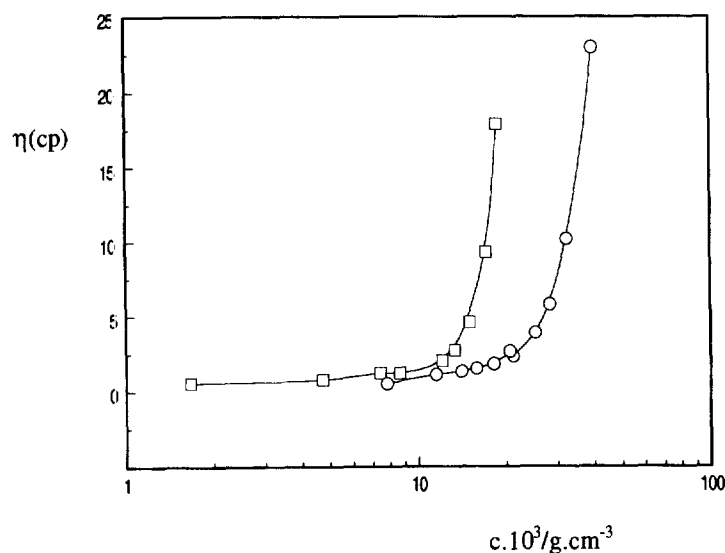


Figure 3 Concentration dependences of the viscosity,  $\eta$ , for the copolymers SEBS1 (○) and SEBS2 (□) in *n*-octane at 25°C

block and with molar masses of  $3.9 \times 10^5$  and  $11.6 \times 10^5 \text{ g mol}^{-1}$  showed radii of gyration of 39 and 32 nm, suggesting that the SEBS micelles in *n*-octane have a more loose or open structure. This different compactness would be caused by the different order degree that both types of micelles would have as mentioned above.

Contrary to the  $M_w$  behaviour, the radius of gyration of the SEBS micelles in *n*-octane decreases as the molar mass of the copolymer increases suggesting that the micelle compactness increases with the copolymer molar mass.

#### Viscosity

The concentration dependences of the viscosity of the copolymer samples SEBS1 and SEBS2 in *n*-octane at 25°C show low and high viscosity, or dilute and semidilute, regions (Figure 3). The cross-over concentrations,  $c^+$ , which divide these low and high slope concentration dependences differ for the two copolymers. For SEBS1  $c^+$

is around  $26 \times 10^{-3} \text{ g cm}^{-3}$ , while for SEBS2 this concentration is  $12 \times 10^{-3} \text{ g cm}^{-3}$ . The lower  $c^+$  shown by the sample SEBS2 suggests that the hydrodynamic radius of the SEBS2 micelles must be larger.

Viscosity extrapolations to zero concentration according to Huggins and Kraemer equations led to different values of the intrinsic viscosity,  $[\eta]$ . The Heller equations were used as alternative extrapolations. The concentration dependences of  $c/\eta_{sp}$  and  $c/\ln \eta_r$  for both copolymers are plotted in Figure 4. The experimental dependences of  $c/\eta_{sp}$  and  $c/\ln \eta_r$  on the concentration were linear within the concentration range employed and the same value of the intrinsic viscosity is obtained from both equations (Table 2).

The linear relationships of viscosity data and concentration found for both copolymers suggest that the hydrodynamic dimensions of the micelles are relatively constant with the concentration. From the slopes the Huggins coefficients,  $k_1$ , were determined, being 0.44 and 0.90 for

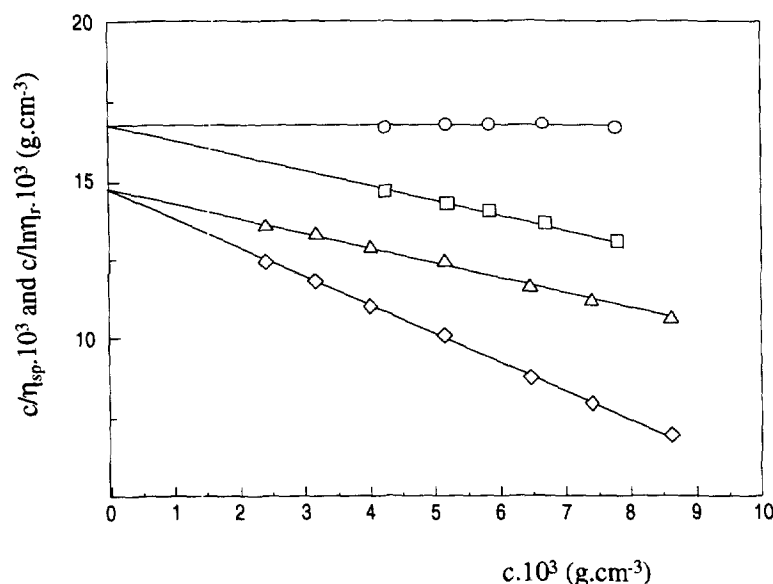


Figure 4  $c/\eta_{sp}$  and  $c/\ln \eta_r$  as a function of concentration for the copolymers SEBS1 ( $\circ$  and  $\square$ ) and SEBS2 ( $\diamond$  and  $\triangle$ ) in *n*-octane at 25°C

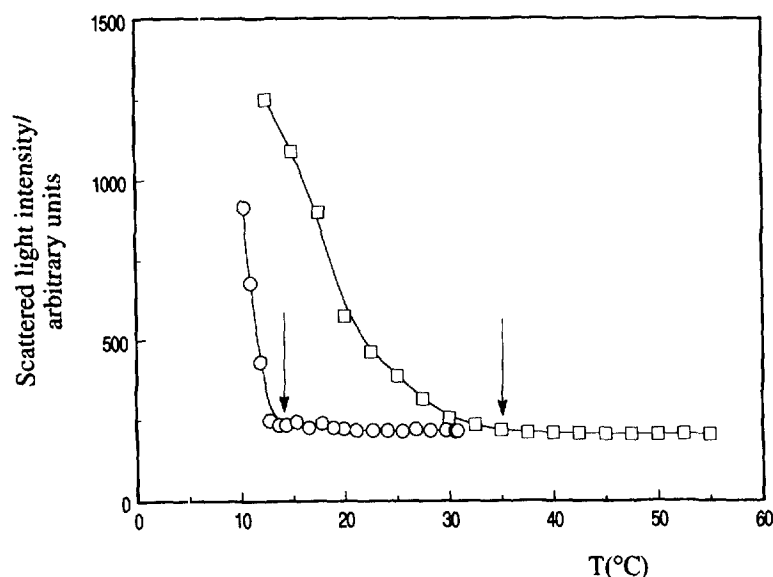


Figure 5 Temperature dependence of the scattered light intensity at a scattering angle of 45° for two SEBS1 ( $\circ$ ) and SEBS2 ( $\square$ ) solutions in *n*-octane.  $c(\text{SEBS1}) = 6.10 \times 10^{-4} \text{ g cm}^{-3}$  and  $c(\text{SEBS2}) = 5.10 \times 10^{-4} \text{ g cm}^{-3}$ .  $\text{CMT}(\text{SEBS1}) = 14^\circ\text{C}$  and  $\text{CMT}(\text{SEBS2}) = 35^\circ\text{C}$

SEBS1 and SEBS2, respectively. These  $k_1$  values are in line with the concept that the larger the Huggins coefficient, the more compact the coil structure is<sup>21</sup>. These data agree with the light scattering results.

The viscometric hydrodynamic radius of the micelles,  $R_\eta$ , was calculated from viscosity and SLS data applying the model of the hydrodynamically equivalent sphere and using Einstein's equation

$$M[\eta] = \nu \frac{4\pi N_A R_\eta^3}{3} = \frac{10\pi N_A R_\eta^3}{3} \quad (8)$$

where  $\nu$  is the shape factor (2.5 for rigid spheres),  $M$  the molar mass and  $N_A$  Avogadro's number. The  $R_\eta$  values obtained are shown in Table 2. Note that  $[\eta]$  belongs to the category of hydrodynamic properties, and thus,  $R_\eta$  is the radius of spheres which are equivalent to the copolymer micelles with respect to their flow behaviour. Here the increment in  $R_h$  with the copolymer molar mass is a

consequence of the increment in the association number and in the length of the copolymer chain.

The intrinsic viscosity is related to the degree of solvation,  $\xi$ , (weight of solvent within the micelle per weight of copolymer) by the equation

$$[\eta] = \frac{\nu}{\rho^*} = \nu(\rho_p^{-1} + \xi\rho_s^{-1}) \quad (9)$$

where  $\rho^*$ ,  $\rho_p$  and  $\rho_s$  are the densities of the particle, polymer ( $0.96 \text{ g cm}^{-3}$ ) and solvent ( $0.70 \text{ g cm}^{-3}$ ), respectively. Equation (9) allows one to determine the degree of solvation (Table 2). These  $\xi$  values must be considered average ones since the micelle core will be very much less solvated than the shell. The values calculated are similar but far higher than those found for the same copolymers in 4-methyl-2-pentanone<sup>20</sup> (1.89 and 2.05 for SEBS1 and SEBS2, respectively). The higher  $\xi$  values found in *n*-octane would be a consequence of the more

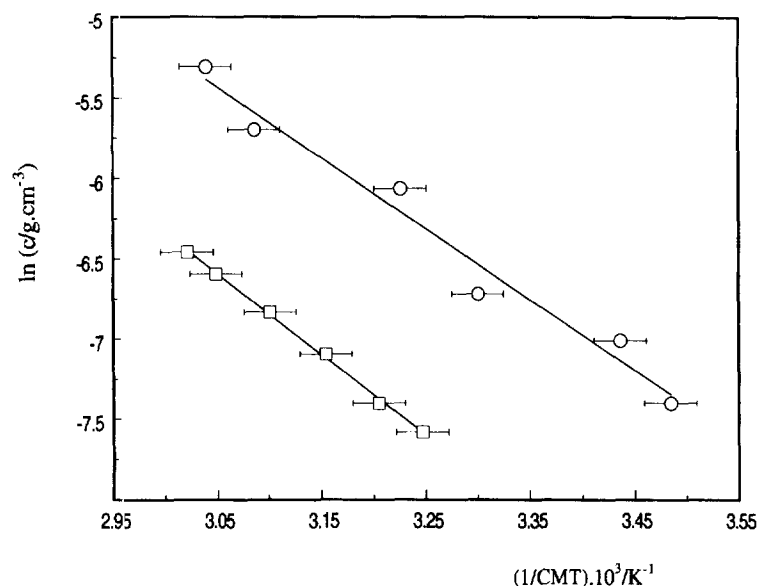


**Figure 6** Plots of the logarithm of the copolymer concentration as a function of the reciprocal of the crucial micelle temperature for the copolymers SEBS1 (O) and SEBS2 (□) in *n*-octane

loose or open structure than these micelles will have which will allow a larger solvent migration into the micelle structure.

#### Thermodynamics functions of micellization

Relationships of concentration and critical micelle temperature for the copolymers SEBS1 and SEBS2 in *n*-octane were determined. In *Figure 5*, light scattering intensity measured at the scattering angle of  $45^\circ$  is plotted as a function of temperature for copolymers SEBS1 and SEBS2 in *n*-octane at concentrations of  $6.1 \times 10^{-4}$  and  $5.1 \times 10^{-4} \text{ g cm}^{-3}$ , respectively. The influence of the temperature on the equilibrium between micelles and unimers controls the plot shape. At the upper end of the temperature range studied only free chains exist while at low temperatures the equilibrium is overwhelmingly in favour of micelle formation. Thus, on lowering the temperature from a high value, a sharp increase in the scattered intensity is observed due to the appearance of micelles.

Critical micelle temperatures were determined for SEBS1 and SEBS2 solutions covering concentrations ranges  $6 \times 10^{-4}$ – $5 \times 10^{-3}$  and  $5 \times 10^{-4}$ – $2 \times 10^{-3} \text{ g cm}^{-3}$ , respectively. All the plots were similar to those shown in *Figure 5*.

Plots of  $\ln c$  as a function of  $(\text{CMT})^{-1}$  for solutions of SEBS1 and SEBS2 in *n*-octane obtained in the basis of Eq. (6) are shown in *Figure 6*. Both plots were linear within the experimental error over the temperatures range studied: 14–60°C for SEBS1 and 35–60°C for SEBS2. The standard Gibbs energy,  $\Delta G^\circ$ , the standard enthalpy,  $\Delta H^\circ$ , and the standard entropy of micellization,  $\Delta S^\circ$ , at 50°C were calculated. These values, per mole of copolymer chain, are shown in *Table 3*. The standard states for micelles and copolymer molecules are states with ideally dilute solutions behaviour and concentration  $1 \text{ mol dm}^{-3}$ .

The standard Gibbs energy of micellization shows negative values for both copolymers, as expected. The copolymer of higher molar mass shows a more negative value of  $\Delta G^\circ$ . Hence, the stability of micelle solutions is higher for longer copolymer chains. This behaviour is similar to that found for the inverse SEBS micelles in 4-methyl-2-pentanone.

**Table 3** Thermodynamic data of the micellization process of SEBS copolymers in *n*-octane at 50°C

	SEBS1	SEBS2
CMC/g cm <sup>-3</sup>	$3.59 \times 10^{-3}$	$1.09 \times 10^{-3}$
$\Delta G^\circ/\text{kJ mol}^{-1}$	-26.2	-30.3
$\Delta H^\circ/\text{kJ mol}^{-1}$	-36.8	-41.9
$T\Delta S^\circ/\text{kJ mol}^{-1}$	-10.6	-11.6

The standard enthalpy of micellization also shows negative values and is solely responsible of the micelle formulation. These negative values are a consequence of the exothermic energy interchange which accompanies the replacement of PS segment/*n*-octane interactions by PS segment/PS segment and *n*-octane/*n*-octane interactions in the formation of the micelle cores. SEBS2 shows a more negative value of  $\Delta H^\circ$  than SEBS1 due probably to the longer PS blocks than SEBS2 has. It is remarkable the less negative values of  $\Delta H^\circ$  values found for the SEBS micelles in *n*-octane compared to the SEBS micelles in 4-methyl-2-pentanone<sup>20</sup> ( $-216$  and  $-204 \text{ kJ mol}^{-1}$  for SEBS1 and SEBS, respectively). This great difference would be a consequence of the looping geometry that the middle poly(ethylene/butylene) block needs to form the micelle. Some polystyrene blocks would come out of the core and would extend into the solution and, on the other hand, the micelles are more solvated as has been seen. Thus, the number of PS/*n*-octane interactions replaced by PS/PS and *n*-octane/*n*-octane interactions will be smaller.

The standard entropy of micellization is also negative for both SEBS copolymers in *n*-octane (*Table 2*) and, therefore, unfavourable to the micellization process. These negative values are due to the increase of the order degree that is associated with the micellization process. Both copolymers show similar  $T\Delta S^\circ$  values. However, these values are far less negative than those corresponding to the entropic contribution to  $\Delta G^\circ$  for SEBS micelles in 4-methyl-2-pentanone ( $T\Delta S^\circ_{50^\circ} = -168$  and  $-147 \text{ kJ mol}^{-1}$  for SEBS1 and SEBS2, respectively). It is clear that the existence of some polystyrene blocks out of the micelle together with the looping geometry of

the middle block will lead to less order in the micelle and therefore to less negative standard entropy of micellization.

#### ACKNOWLEDGEMENTS

M.D.J. thanks the Departamento de Educación, Universidades e Investigación of Gobierno Vasco, for her grant. We also thank the CYTED (Programa Iberoamericano de Ciencia y Tecnología para el Desarrollo) for their financial support.

#### REFERENCES

1. Brown, R. A., Masters, A. J., Price, C. and Yuan, X. F., *Comprehensive Polymer Science*, Vol. 2, ed. G. Allen and J. C. Bevington, Pergamon Press, Oxford, 1989, Chapter 6.
2. Quintana, J. R., Villacampa, M. and Katime, I., *Rev. Iberoamer. Polim.*, 1992, **1**, 5.
3. Tuzar, Z. and Kratochvil, P., *Surface and Colloid Science*, Vol. 15(1), ed. E. Matijevic, Plenum Press, New York, 1993.
4. Quintana, J. R., Villacampa, M. and Katime, I., in *The Polymeric Materials Encyclopedia*, ed. J. C. Salamone, CRC Press, in press.
5. Candau, F., Heatley, F., Price, C. and Stubbersfield, R. B., *Eur. Polym. J.*, 1984, **20**, 685.
6. Price, C., Stubbersfield, R. B., El-Kafrawy, S. and Kendall, K. D., *British Polym. J.*, 1989, **21**, 391.
7. Tanaka, T., Kotaka, T. and Inagaki, H., *Polym. J.*, 1972, **3**, 327.
8. Tanaka, T., Kotaka, T. and Inagaki, H., *Polym. J.*, 1972, **3**, 338.
9. Tang, W. T., Hadziioannou, G., Cotts, P. M., Smith, B. A. and Frank, C. W., *Polym. Prepr. (Am. Chem. Soc., Div. Polym. Chem.)*, 1986, **27**(2), 107.
10. Plestil, J., Hlavatá, D., Hronz, J. and Tuzar, Z., *Polymer*, 1990, **31**, 2112.
11. Balsara, N. P., Tirrell, M. and Lodge, T. P., *Macromolecules*, 1991, **24**, 1975.
12. Quintana, J. R., Jáñez, M. D. and Katime, I., *Langmuir*, submitted for publication.
13. Tuzar, Z., Konak, C., Stepanek, P., Plestil, J., Kratochvil, P. and Prochazka, K., *Polymer*, 1990, **31**, 2118.
14. Bahadur, P., Sastry, N. V., Marti, S. and Riess, G., *Colloids Surf.*, 1985, **16**, 337.
15. Bluhm, T. and Malhotra, S. L., *Eur. Polym. J.*, 1986, **22**, 249.
16. Price, C., Chan, E. K. and Stubbersfield, R. B., *British Polym. J.*, 1989, **21**, 391.
17. Quintana, J. R., Villacampa, M., Salazar, R. and Katime, I., *J. Chem. Soc., Faraday Trans.*, 1992, **88**, 2739.
18. Xu, R., Winnik, M. A., Riess, G., Chu, B. and Croucher, M. D., *Macromolecules*, 1992, **25**, 644.
19. Quintana, J. R., Villacampa, M. and Katime, I., *Makromol. Chem.*, 1993, **194**, 983.
20. Villacampa, M., Quintana, J. R., Salazar, R. and Katime, I., *Macromolecules*, 1995, **28**, 1025.
21. Lovell, P. A., *Comprehensive Polymer Science*, Vol. 1, ed. C. Booth and C. Price, Pergamon Press, Oxford, 1989, Chapter 9.
22. Price, C., *Pure Appl. Chem.*, 1983, **55**, 1563.
23. Price, C., Booth, C., Canham, P. A., Naylor, T. V. and Stubbersfield, R. B., *British Polym. J.*, 1984, **16**, 391.
24. Katime, I. and Quintana, J. R., *Comprehensive Polymer Science*, Vol. 1, ed. C. Booth and C. Price, Pergamon Press, Oxford, 1989, Chapter 5.